



## CHAPTER II

### HYDROPHOBIC CHAIN CONJUGATION AT HYDROXYL GROUP ONTO $\gamma$ -RAY IRRADIATED CHITOSAN

#### Abstract

$\gamma$ -Ray irradiation of chitosan flakes and introduction of hydrophobic chains onto hydroxyl groups are discussed. At 25 kGy, chain degradation without crosslinking reduces the molecular weight to one-fourth, however structural characterization by FT-IR,  $^1\text{H-NMR}$ , and  $^{13}\text{C}$  CP/MAS NMR indicates that the saccharide units are maintained. Introduction of hydrophobic chains is accomplished by introduction of alkyl amine group onto the chitosan carbonyl imidazole precursor. The chitosan coupling reaction is improved and can be done homogeneously as a result of  $\gamma$ -ray irradiation. The optimum conditions for phthalimido group deprotection are studied to generate a unique product with a hydrophobic chain attached mainly at hydroxyl group (C-6 and/or C-3) while amino group (C-2) is retained as characterized by FT-IR, and  $^1\text{H-NMR}$ . The final product shows fair solubility in organic solvents, such as DMSO, DMAc, DMF, and pyridine.

## Introduction

Chitin-chitosan is the second most naturally abundant copolysaccharide of  $\beta$ -(1-4)-2-acetamido-2-deoxy- $\beta$ -D-glucose and  $\beta$ -(1-4)-2-amino-2-deoxy- $\beta$ -D-glucose (Scheme 1). Due to its specific properties including biocompatibility<sup>1,2</sup>, biodegradability<sup>3,4</sup>, bioactivity<sup>5,6</sup>, and non-toxicity and the potential for physical<sup>7,8</sup> and chemical<sup>9-13</sup> modification, chitin-chitosan has received much interest as a precursor to value added biopolymers. Structural modification of chitin-chitosan by reaction with other functional groups has been proposed as a route to derivatives for advanced applications<sup>14,15</sup>. Owing to the high molecular weight and strong intra- and intermolecular hydrogen bonds, the structural modification of chitin-chitosan by chemical reactions is limited. To break through this problem, an alternate way is to first reduce its molecular weight to access to the reactive functional groups or provide access for chemical species to react with the chitin-chitosan chain effectively.

Chemical treatment<sup>16-18</sup>, enzymatic degradation<sup>19,20</sup>, and photoirradiation<sup>21-24</sup> are all pathways for chain degradation of chitin-chitosan. Although chemical treatment can be easily done, the amount of consumed acid/base and the waste are of concern. Enzymatic degradation can be achieved under mild conditions; however, using multi-step procedures. Photoirradiation with  $\gamma$ -rays is an effective pathway when we consider that it is a single-step procedure that allows extensive modification without waste. Although some studies of  $\gamma$ -ray irradiation of polysaccharides have been done previously, the chemical modification of  $\gamma$ -ray irradiated polysaccharide is rarely seen. It is important to answer the question whether chitosan, following  $\gamma$ -ray irradiation; maintains its structure before using it as a starting material for further chemical modification. Ebringerova et al.<sup>25</sup> reported that  $\gamma$ -ray irradiation for solid arabinoxylan induced changes in sugar composition, formation of new functional groups, cleavage of glycosidic bonds, decreases in molecular weight, and increases in water solubility. Chen et al.<sup>26</sup> reported that the glycoside linkages of cellulose triacetate were degraded to carbonyl and carboxyl species at chain termini.

Regarding chitosan modification, the introduction of hydrophobic groups is an attractive objective, especially when aiming for the complexation and/or

aggregation of hydrophobic chitosan with specific molecules, i.e., drugs, pesticides, or toxic reagents through micelle formation. The chitosan structure contains amino and hydroxyl groups that are useful for chemical modification. Owing to the higher reactivity of the amino group at C-2 than the hydroxyl groups at C-6 and C-3, most studies on the chemical modification of chitosan deal with reactions at the amino group. In the case of hydrophobic chain functionalization, Miwa et al.<sup>27</sup> proposed forming lauryl chains on the amino groups of carboxymethyl chitosan. Yoshioka et al.<sup>28</sup> reported a series of sulfated *N*-acyl-chitosans possessing various alkyl chain lengths at the C-2 unit. However, when we consider the unique structure of chitosan, it is important to maintain the aminosaccharide unit for specific properties. In another words, if chitosan with a hydrophobic chain only at hydroxyl groups can be realized, the properties of the aminosaccharide groups will be retained.

The present work focuses on the effective functionalization of hydroxyls with hydrophobic groups by using reduced molecular weight chitosan obtained from  $\gamma$ -ray irradiation processes. In the first step, we determine the optimum  $\gamma$ -ray irradiation conditions to obtain molecular weight reduction with minor changes in the structure of the product. In the second step, the  $\gamma$ -ray irradiated chitosan is coupled with a spacer group for further functionalization with a hydrophobic chain. The present work is unique in terms of the final product with a hydrophobic group selectively added at C-6 and/or C-3.

## Experimental

### Chemicals

Chitosan with 81.8% deacetylation (Scheme 1,  $x = 81.8$ ) was provided by the Asian Institute of Technology (AIT), Bangkok, Thailand. *N,N'*-Carbonyldiimidazole (CDI) was obtained from TCI, Japan. Methanol was purchased from J.T. Baker, USA. Acetic acid, *N,N*-dimethylformamide (DMF), and sodium hydroxide were supplied by UNIVAR, Australia. Phthalic anhydride, *n*-hexylamine, and deuterium oxide were purchased from Fluka Chemika, Switzerland. Ethanol, and acetone were obtained from BDH Laboratory Supplies, England. Sodium acetate was purchased from Wako Pure Chemical Industries, Ltd.,

Japan. Hydrazine monohydrate was purchased from Nacalai Tesque., Inc., Kyoto, Japan. Acetic acid-d<sub>4</sub> was obtained from GROUPE cea C.E SACLAY, France. Methyl sulfoxide-d<sub>6</sub> was purchased from Aldrich. All chemicals were used without further purification.

### Instruments and Equipment

Qualitative and quantitative FT-IR spectra were recorded on a VECTOR 3.0 BRUKER spectrometer with 64 scans at a resolution of 4 cm<sup>-1</sup> using a deuterated triglycinesulfate detector (DTGS) with a specific detectivity, D\*, of 1x10<sup>9</sup> cm.Hz<sup>1/2</sup>w<sup>-1</sup>. <sup>13</sup>C CP/MAS NMR spectra were taken at 300 MHz with a BRUKER DPX-300 at 23±1°C. Degree of deacetylation (DD) was analyzed by the acid hydrolysis-HPLC method.<sup>29</sup> The analysis of acetic acid was carried out using a Waters HPLC with a 300 x 7.8 mm column ORH-801 cation exchange resin (Interaction Chromatography INC., 2032 Concourse Drive, San Jose, CA 95131); 1 mM H<sub>2</sub>SO<sub>4</sub>; flow rate 0.8 mL/min; pressure 1600 psi; He degas at rate of 15 mL/min; column oven temperature 45°C; sample compartment 25°C; injection volume 30μL; detection at 210 nm by a Waters<sup>TM</sup> 486 Tunable absorbance detector. <sup>1</sup>H-NMR spectra were obtained using a JEOL GSX 400 (400 MHz) at 70±1°C. Powder X-ray diffraction patterns were recorded over a 2θ range of 5-50° by a RIGAKU RINT 2000 using CuKα as an X-ray source and operating at 40 kV, 30 mA with Ni filter. Elemental analyses were obtained using a YANAKO CHN CORDER MT-3, MT-5 Analyzer with a combustion temperature at 950°C under air with O<sub>2</sub> as a combustion gas (flow rate 20 mL/min) and He as a carrier (flow rate 200 mL/min). A Dupont thermogravimetric analyzer was used for TGA studies using an N<sub>2</sub> flow rate of 20 mL/min and a heating rate of 20°C/min from 30° to 600°C. Intrinsic viscosity [η] of chitosan and γ-ray irradiated chitosan samples as measured with a calibrated viscometer Cannon-Ubbelohde (NO 2, A149) in 0.2 M CH<sub>3</sub>COOH/0.1 M CH<sub>3</sub>COONa aqueous solution at 30 ± 0.05°C. Molecular weight was calculated using the Mark-Houwink equation with K = 9.8490 x 10<sup>4</sup> mL/g, and a = 0.9856.<sup>30</sup> A Lamda-10 UV-VIS spectrophotometer from Perkin-Elmer was used to study the structural change of chitosan after γ-ray irradiation.

## Procedures:

### $\gamma$ -Ray Irradiated Chitosan

$\gamma$ -Ray irradiation was carried out in a  $\gamma$ -cell (Co-60) courtesy of the Office of Atomic Energy for Peace (OAEP), Ministry of Science and Technology, Thailand. Dried flake samples were irradiated in air at various doses up to 96.23 kGy, at a dose rate of 6.88 kGy/h.

### Chemical Modification of $\gamma$ -Ray Irradiated Chitosan

$\gamma$ -Ray irradiated chitosan, **1** (1.00 g) was reacted with phthalic anhydride (4.39 g, 5 moles equivalent to pyranose rings) in *N,N*-dimethylformamide (DMF) (20 mL) at 100°C under nitrogen for 6 h. The temperature was reduced to 60°C and the mixture was left overnight. Decanted solution was concentrated and product reprecipitated in ice water. The precipitate was collected, washed with ethanol three times, and dried in vacuo to give pale yellow **2** (Scheme 2).

Anal. Calcd. for  $(C_{14}H_{13}O_6N)_{0.69} (C_6H_{11}O_4N)_{0.13} (C_8H_{13}O_5N)_{0.18}$ : (%) C, 55.24; H, 4.94; and N, 5.42. Found: (%) C, 55.13; H, 4.45; and N, 3.35: FT-IR (KBr,  $cm^{-1}$ ) 3472 (OH), 1776 and 1714 (C=O anhydride), and 721 (aromatic ring):  $^{13}C$  CP/MAS NMR ( $\delta$ , ppm) 23.3 (CH<sub>3</sub>), 57.0 (C-2), 64.7 (C-6), 73.2 (C-3, C-5), 80.5 (C-4), 100.4 (C-1), 131.1 (aromatic ring), and 169.1 (C=O):  $^1H$ -NMR ( $\delta$ , ppm) 1.7 (CH<sub>3</sub> in acetamide), 3.4-5.0 (pyranose ring), and 7.6-7.7 (aromatic ring).

Compound **2** (1.00 g) was dispersed in DMF (20 mL) and heated to 100°C in vacuo. After 30 min, *N,N'*-Carbonyldiimidazole (CDI) (1.79 g, 3 moles equivalent to pyranose rings) was added and reacted at 100°C for 30 min. The temperature was reduced to 60°C and stirring was continued for 2 h. The mixture obtained was concentrated and precipitated using acetone. The precipitate was rinsed with acetone and dried in vacuo to give **3** (Scheme 2).

Anal. Calcd. for  $(C_{18}H_{15}O_7N_3)_{0.69} (C_{14}H_{15}O_6N_5)_{0.13} (C_{12}H_{15}O_6N_3)_{0.18}$ : (%) C, 53.99; H, 4.12; and N, 12.52. Found: (%) C, 54.49; H, 4.66; and N, 9.45: FT-IR (KBr,  $cm^{-1}$ ) 3474 (OH), 1776 and 1714 (C=O anhydride), 1774 (C=O in reactive ester), and 721 (aromatic ring):  $^{13}C$  CP/MAS NMR ( $\delta$ , ppm) 124.1 and 134.7

(imidazole):  $^1\text{H-NMR}$  ( $\delta$ , ppm) 1.7 ( $\text{CH}_3$  in acetamide), 3.2-5.2 (pyranose ring), 7.0 (imidazole), and 7.6-7.8 (aromatic ring).

The reaction of alkyl amine with the chitosan precursor was achieved as follows. Compound **3** (1.00 g) was dissolved in DMF (20 mL) at  $70^\circ\text{C}$  in vacuo. After 1 h, *n*-hexylamine (1.3 mL, 3.36 moles equivalent to pyranose rings) was added and the reaction was carried out at  $70^\circ\text{C}$  for 3 h. The reaction was continued overnight under nitrogen. The solution was concentrated and precipitated with acetonitrile. The precipitate was collected and washed thoroughly with acetonitrile, followed by drying in vacuo to give a pale yellow powder **4** (Scheme 2).

Anal. Calcd. for  $[(\text{C}_{21}\text{H}_{26}\text{O}_7\text{N}_2)_{0.69} (\text{C}_{20}\text{H}_{37}\text{O}_6\text{N}_3)_{0.13} (\text{C}_{15}\text{H}_{26}\text{O}_6\text{N}_2)_{0.18}]_{0.75} [(\text{C}_{14}\text{H}_{13}\text{O}_6\text{N})_{0.69} (\text{C}_6\text{H}_{11}\text{O}_4\text{N})_{0.13} (\text{C}_8\text{H}_{13}\text{O}_5\text{N})_{0.18}]_{0.25}$ : (%) C, 58.41; H, 6.49; and N, 7.07. Found: (%) C, 56.49; H, 7.13; and N, 6.64: FT-IR (KBr,  $\text{cm}^{-1}$ ) 3125-3725 (OH), 2862-3071 (C-H), 1776, and 1714 (C=O of anhydride), 1714 (carbamate bond) and 721 (aromatic ring):  $^1\text{H-NMR}$  ( $\delta$ , ppm) 0.8 ( $\text{CH}_3$ ), 1.2 ( $\text{CH}_2$ ), 1.7 ( $\text{CH}_3$  in acetamide), 3.4-5.1 (pyranose ring), and 7.5 (aromatic ring).

Compound **4** (1.00 g) was stirred in DMF (20 mL) and heated to  $100^\circ\text{C}$  under nitrogen. Hydrazine monohydrate was added and the reaction was continued for 1 h. The yellow solution was allowed to cool to room temperature resulting in precipitation. The precipitate was collected and washed thoroughly with methanol and dried in vacuo to yield **5** (Scheme 2).

Anal. Calcd. for  $[(\text{C}_{13}\text{H}_{24}\text{O}_5\text{N}_2)_{0.69} (\text{C}_{20}\text{H}_{37}\text{O}_6\text{N}_3)_{0.13} (\text{C}_{15}\text{H}_{26}\text{O}_6\text{N}_2)_{0.18}]_{0.73} [(\text{C}_{10}\text{H}_{13}\text{O}_5\text{N}_3)_{0.69} (\text{C}_{14}\text{H}_{15}\text{O}_6\text{N}_5)_{0.13} (\text{C}_{12}\text{H}_{15}\text{O}_6\text{N}_3)_{0.18}]_{0.02} [(\text{C}_6\text{H}_{11}\text{O}_4\text{N})_{0.82} (\text{C}_8\text{H}_{13}\text{O}_5\text{N})_{0.18}]_{0.25}$ : (%) C, 53.23; H, 8.03; and N, 9.51. Found: (%) C, 48.26; H, 7.62; and N, 8.09: FT-IR (KBr,  $\text{cm}^{-1}$ ) 3125-3725 (OH), 2862-3071 (C-H), 1714 (carbamate bond) and 1150 ( $\text{NH}_2$ ):  $^1\text{H-NMR}$  ( $\delta$ , ppm) 0.8 ( $\text{CH}_3$ ), 1.2 ( $\text{CH}_2$ ), 1.7 ( $\text{CH}_3$  in acetamide), 3.4-5.1 (pyranose ring), and 7.4 (aromatic benzene ring).

## Results and Discussion

### $\gamma$ -RAY IRRADIATED CHITOSAN

#### $\gamma$ -Ray Irradiation Effect on Molecular Weight

In the present work, high molecular weight chitosan flake (%DD = 81.8,  $M_v = 2.2 \times 10^6$ ) was irradiated in air over a wide range of  $\gamma$ -ray dosages to observe changes in molecular weight and chemical structure. Molecular weight evaluated via intrinsic viscosity decreased significantly to one-fourth when  $\gamma$ -ray dose is 25 kGy (Figure 1). Ulanski et al.<sup>22</sup> reported that  $\gamma$ -ray irradiation of solid chitosan (%DD = 91.0,  $M_w = 1.4 \times 10^6$ ) in air gave the molecular weight reduction to one-third at 25 kGy. The difference in molecular weight reductions may be due to chitosan source, degree of deacetylation, and crystallinity. In our work, it was found that the molecular weight was rather stable at  $M_v = 5.2 \times 10^5$  corresponding to  $3 \times 10^3$  mers after 25 kGy irradiation. This might be due to the semi-crystalline chitosan structure. Initially,  $\gamma$ -ray irradiation may affect amorphous regions leading to significant reduction in molecular weight. When the amorphous regions are destroyed, irradiation energy only then begins to degrade the crystalline segments. However, even at high doses, the effect of irradiation on the crystalline portion was less since it is difficult to break the tightly packed chains. This could be confirmed by structural analysis, as summarized in the next section. As a result, the molecular weight reduction did not change above a certain dose level. It was found that the product changed from white to yellow in color. The mechanism of solid state chitosan degradation by  $\gamma$ -ray irradiation was reported previously to involve chain scission as radical species are generated at C-1 and/or C-4.<sup>31</sup> These species induce chain scission at the 1,4-glycosidic bond. In contrast, if radical species form at other carbons, crosslinking will occur and the molecular weight should increase. In our case, the obtained product dissolved completely in acetic acid to a clear solution. This implies that  $\gamma$ -ray irradiation of chitosan solid flakes induces chain degradation without crosslinking.

### **$\gamma$ -Ray Irradiation Effect on Saccharide Unit**

In the present work, FT-IR,  $^1\text{H-NMR}$ ,  $^{13}\text{C CP/MAS NMR}$  and UV techniques were applied to clarify the changes in structure. The FT-IR peaks at  $895\text{-}1200\text{ cm}^{-1}$  of each  $\gamma$ -ray irradiated chitosan sample obtained at various doses suggest that the saccharide backbone is maintained (Figure 2).  $\gamma$ -Ray irradiated chitosan at different doses show similar  $^1\text{H-NMR}$  patterns. The peak at  $1.8\text{ ppm}$  arises from the methyl protons, while the peaks at  $2.9\text{-}4.7$  can be assigned to protons of each carbon in the hexosamine unit.  $^{13}\text{C CP/MAS NMR}$  spectra of  $\gamma$ -ray irradiated chitosan obtained at various doses also show similar patterns to unirradiated materials (Table 1). The signals due to carbons of hexosamine residues are assigned at  $57.7\text{-}105.3\text{ ppm}$ . The single peak at  $24.0\text{ ppm}$  is assigned to methyl protons while the  $174.0\text{ ppm}$  peak is assigned to the  $\text{C=O}$  acetamide. Wenwei et al.<sup>24</sup> reported that the glycosidic bonds ( $\text{C}_1\text{-O-C}_4$  group) decrease with increasing radiation doses leading to hydroxyl group formation as observed by FT-IR. In the present work, the change in hydroxyl group intensity was evaluated by FT-IR using the peak intensity ratio at  $3582\text{ cm}^{-1}$  (hydroxyl band) and  $1655\text{ cm}^{-1}$  (amide I band). It should be noted that the change in hydroxyl groups is insignificant and not related to the  $\gamma$ -ray dosage. However, further studies by UV-VIS spectroscopy (Figure 3) indicate that the carbonyl peak at  $293\text{ nm}$  increases significantly. Thus, chain degradation might occur mainly at glycoside linkages to generate some carbonyl terminal groups as proposed by Ulanski et al.<sup>22</sup>. Taking all structural characterization results into consideration, we conclude that although the molecular weight was reduced significantly, most saccharide units still remain. Here, the  $\gamma$ -ray dosage at  $25\text{ kGy}$  was chosen as optimal for  $\gamma$ -ray irradiated chitosan raw material to be used for further processing.

### **$\gamma$ -Ray Irradiation Effect on Morphology and Degree of Deacetylation**

Powder X-ray diffraction was used to study the changes in packing structure after  $\gamma$ -ray irradiation. The patterns of  $\gamma$ -ray irradiated chitosan at various doses were the same as those of the starting material with the peaks at lattice angles of  $9.7^\circ$  and  $19.8^\circ\ 2\theta$  (Figure 4). This suggests that  $\gamma$ -ray irradiation up to  $96.23\text{ kGy}$  does



not affect chitosan crystallinity.

The effect of  $\gamma$ -rays on degrees of deacetylation was evaluated by a curve fitting quantitative FT-IR technique using the peak ratio of the amide I band ( $1655\text{ cm}^{-1}$ ) and hydroxyl band ( $3450\text{ cm}^{-1}$ ). The results point out that the degree of deacetylation is maintained at a ratio of 0.15 (Figure 5). This is confirmed by direct evaluation methods, i.e.,  $^1\text{H-NMR}$  and acid hydrolysis-HPLC techniques as shown in Figure 5. The evaluation from both methods support measured degree of deacetylation as being constant at  $0.81 \pm 0.01$  for each  $\gamma$ -ray dose. This confirmed that the chain degradation by  $\gamma$ -ray irradiation occurs at random positions and has no effect on the degree of deacetylation.

## **CHEMICAL MODIFICATION OF $\gamma$ -RAY IRRADIATED CHITOSAN**

### **Comparable Studies on Reactivity of $\gamma$ -Ray Irradiated Chitosan and Unirradiated Chitosan**

The preliminary reaction with CDI was chosen to compare the reactivity of unirradiated and  $\gamma$ -ray irradiated chitosan (at 25 kGy) since the reaction can be qualitative and quantitative by FTIR. Figure 6 demonstrates that both products give the characteristic peak of a reactive ester at  $1745\text{ cm}^{-1}$  (Figure 6). The ratio of the carbonyl (carbonyl imidazolide) band at  $1745\text{ cm}^{-1}$  to the pyranose band at  $897\text{ cm}^{-1}$  as derived from curve fitting FT-IR technique was applied to quantitate the degree of CDI substitution. The integral ratios of the product coupling with CDI were found to be 2.5, and 1.6 for  $\gamma$ -ray irradiated and unirradiated chitosan, respectively. This means that  $\gamma$ -ray irradiation enhances the reactivity of chitosan by 50-60%. In another words, the decrease in molecular weight after  $\gamma$ -ray irradiation is the key factor improving chitosan reactivity.

### **Protection of Amino Group on $\gamma$ -Ray Irradiated Chitosan**

Though several reports on  $\gamma$ -ray irradiated chitosan have been published, the chemical reactions of  $\gamma$ -ray irradiated products are rarely discussed. In this work, we focused on chain modification of  $\gamma$ -ray irradiated chitosan under the conditions where reaction occurs mainly at hydroxyl groups while amino groups

remained unreacted. In order to achieve this goal, protection of the amino group with phthalic anhydride<sup>10</sup> was carried out in a first step.

Figure 2 clarifies that the  $\gamma$ -ray irradiated chitosan after reaction with phthalic anhydride shows the phthalimido characteristic peaks at 1776 and 1714  $\text{cm}^{-1}$  referring to carbonyl anhydride and 721  $\text{cm}^{-1}$  belonging to aromatic ring.  $^{13}\text{C}$  CP/MAS NMR summarized in Table 1 clarifies the aromatic ring in phthalimido group as a single sharp peak at 131.1 ppm, and two types of C=O belonging to acetamide and phthalimido groups at 169.1 ppm. In addition,  $^1\text{H}$ -NMR also supported the successful phthaloylation as seen from the peak at 7.6 ppm belonging to protons of the phenyl ring. The degree of phthaloylation evaluated by elemental analysis was found to be 84 %.

Thermogravimetry analyses were used to evaluate thermal stability of the derivatives obtained. For  $\gamma$ -ray irradiated chitosan, **1**, TG /DTA shows mass losses at 58° and 320°C, revealing the loss of moisture and then chitosan degradation, respectively. However, N-phthaloyl  $\gamma$ -ray irradiated chitosan, **2**, gave an endothermic peak at 220°C that can be assigned to phthalimido groups. From these results, it can be concluded that the phthalimido group was successfully introduced onto  $\gamma$ -ray irradiated chitosan. The XRD pattern of **2** shows a broad peak at 19°  $2\theta$  (Figure 4). This might relate to the reduction of inter- and intramolecular hydrogen bonds of chitosan chain by the bulky phthalimido groups. Compound **2** was found to be dissolve easily in organic solvents such as DMF, DMSO, DMAc and pyridine. This provides the homogeneous systems for chemical modification in the next step.

### **$\gamma$ -Ray Irradiated Chitosan Precursor**

In the present work, *N,N'*-carbonyldiimidazole (CDI) was chosen as a coupling agent due to its high reactivity with alcohols, carboxylic acids, and amines, which are important functional groups in carbohydrate polymers. Because of the electron attraction exerted from both sides on the carbonyl group by the heterocyclic ring, the CDI reacts easily via nucleophilic substitution for which both hydroxyl and amino groups can act as nucleophiles.<sup>32,33</sup> Here, most of the amino groups at C-2 were protected by phthalic anhydride in the first step to avoid reaction with CDI.

According to the high reactivity of CDI, the reaction has run in a non-aqueous system to control the degradation. In our previous work<sup>13</sup>, the reaction was run in a heterogeneous system and the yield was low. Compound **2** is expected to provide high yields since it is soluble in DMF allowing homogeneous reaction system.

Compound **2** reacted with CDI for the reactive ester imidazole as seen by FT-IR (Figure 2), peaks at  $1774\text{ cm}^{-1}$  for reactive ester imidazole and at  $1714\text{ cm}^{-1}$  for a carbamate appear.  $^{13}\text{C}$  CP/MAS NMR (Table 1) and  $^1\text{H}$ -NMR show new peaks due to imidazole group at 124.2 and 134.7 ppm, and 7.02 ppm, respectively. This confirms the success of the reaction to form compound **3**. The degree of substitution was 75 % as determined by C/N ratio. It should be noted that CDI substitution takes place at the C-6 and C-3 hydroxyl groups, as confirmed by  $^{13}\text{C}$  CP/MAS NMR (Table 1). By comparing the chemical shift of **3** to that of **2**, the peaks at 64.6, and 73.2 ppm belonging to C-6, and C-3, respectively were split into doublets implying that CDI substitution occurred predominantly at C-6, and partially at C-3.

Thermal stability studied by TG/DTA revealed four endotherms as compared to **2**. The endotherm at  $195^\circ\text{C}$  points to the loss of imidazolide, while the one at  $262^\circ\text{C}$  reflects the loss of phthalimido group. Figure 4 reveals the packing structure of **3** for the increase in crystallinity comparing to **2** as confirmed by the change in the peak at  $22^\circ 2\theta$ . This implies that the reactive ester group induces other types of chain packing, which might be due to intramolecular hydrogen bonding between the carbamate and chitosan hydroxyl groups. As a result, the solubility of **3**, especially in DMF, DMSO, DMAc, and pyridine decreases significantly as compared to **2** (Table 2).

### **Conjugation of $\gamma$ -Ray Irradiated Chitosan Precursor with Alkyl Amine and Protecting Group Removal**

In the present work, alkyl amine functionalization of **3** using n-hexylamine in DMF was attempted. After 3 h, the reactive ester imidazole groups are consumed as evidenced by disappearance of the peak at  $1774\text{ cm}^{-1}$  (Figure 2). The peaks at  $1776\text{ cm}^{-1}$  (C=O anhydride), and at  $1714\text{ cm}^{-1}$  (C=O anhydride and

carbamate) confirm the structure of **4** (Scheme 2). New peaks at 2800-3100  $\text{cm}^{-1}$  for  $^{\nu}\text{C-H}$  appeared significantly implying the successful addition of the hydrophobic chain.  $^1\text{H-NMR}$  also confirms the introduction of hexyl chains onto **3** as characterized by peaks at 0.8 ppm (methyl proton), 1.2 ppm (methylene proton), and a diminished peak at 7.0 ppm (imidazole proton). This suggests that substitution onto **3** is almost complete. However, during the substitution of hexyl amine, moisture likely competed for reaction with the reactive spacer, as a result, the substitution was not 100%. This might be one reason that the substitution of n-hexylamine was around 73 %, as determined from C/N ratio.

Considering the structure of **4**, it can be hypothesized that the hydrophobicity might relate to the N-phthaloyl group and the hexyl chains in each chitosan unit. However, the deprotection of the N-phthaloyl group to obtain amino group could bring a hydrophilic site back to chitosan as shown in **5**. The removal of N-phthaloyl group by hydrazine may occur at both phthalimide and carbamate bonds. Thus, we faced an important point of controlling the removal of the phthalimido group. The optimum conditions for removing phthaloyl group were determined. In the present work, the reaction was carried out homogeneously in DMF at 100°C under nitrogen for 1 h to selectively deprotect the phthalimido group.

The FT-IR of **5** (Figure 2) shows the peak at 721  $\text{cm}^{-1}$  (phenyl ring) has almost disappeared, while the peak at 1150  $\text{cm}^{-1}$  (amino group) appears, in addition, the peaks at 2800-3100  $\text{cm}^{-1}$  (methylene groups) still exist. It should be noted that hydrazine can react at either the phthalimide bond to give an amino group and/or at the hexyl carbamate bond to give a carbamate amino group as shown in Scheme 2. If both cases, **5** should reveal a urethane peak. Here, the product suggests that **5** retains the carbamate bond at 1714  $\text{cm}^{-1}$  which might be related to urethane hexyl group ( $-\text{OCONH}(\text{CH}_2)_5\text{CH}_3$ ) and/or urethane amino group ( $-\text{OCONHNH}_2$ ).  $^1\text{H-NMR}$  strongly revealed the existence of urethane hexyl group as identified from the peaks at 0.8 ppm (methyl proton) and 1.2 ppm (methylene proton). This implies that the added hexyl group was not removed by hydrazine. The  $^1\text{H-NMR}$  data suggest that incomplete deprotection occurred since the aromatic phthalimido peaks at 7.4 ppm still remained. The C/N ratio from elemental analysis indicated

deprotection was 82 % effective.

It is important to clarify the reason why deprotection of the phthalimide was the primary reaction rather than reduction of the hexyl carbamate. The selective deprotection at phthalimide might be due to the fact that the phthalimido group impedes chitosan chain packing. It might also be related to the high degree of substitution of the hexyl groups in the previous step, since the effective reaction occurred owing to reduced intermolecular hydrogen bonding via  $\gamma$ -ray irradiation. Thus, a number of hexyl chains pack closes together and hydrazine was unable to penetrate this hydrophobic environment to effect reaction in good yield. In another words, the reaction of hydrazine at the phthalimido group was easy relative to at the hexyl group. This leads to the selective substitution of hexyl chains at hydroxyl groups and the remaining specific amino groups on the chitosan chain.

### **Performance of $\gamma$ -Ray Irradiated Chitosan with a Hexyl Chain at Hydroxyl Groups**

As amino group at C-2 is more reactive than the hydroxyl groups at C-6 and C-3, the selective reaction at the hydroxyls achieved here is very important and unique. It is expected that the final product will show the overall performance of chitosan but with high hydrophobicity. In this step, we focused on the solubility and/or swelling ability of chitosan in various organic solvents as summarized in Table 2. Theoretically, the solubility characteristics of compounds depend mainly on their polarity and in particular on their hydrogen bonding ability.<sup>34</sup> Complete dissolution can be expected when the solubility parameters and the degree of hydrogen bonding are similar between the two components, i.e., solute and solvent<sup>35</sup>. Here, the final product will dissolve easily in organic solvents with a solubility parameter ( $\delta$ ) 12.0-12.1 (cal/cm<sup>3</sup>)<sup>1/2</sup>, i.e., DMF and DMSO. The effective introduction of a hydrophobic group in **5** leads to the reduction of intermolecular forces, and the destruction of the tight packing of the rigid polysaccharide molecules.

## Conclusion

$\gamma$ -Ray irradiation is a very practical pathway for decreasing the molecular weight of chitosan. At certain doses of  $\gamma$ -rays, molecular weights can be reduced with only slight changes in structure. The reactivity of  $\gamma$ -ray irradiated chitosan was enhanced as clarified by the model reaction with carbonyldiimidazole. High yield functionalization of hexyl chains onto chitosan was successful due to solubilization. The deprotection of a phthalimide group at C-2 occurred selectively to give an aminosaccharide with a hydrophobic chain on the hydroxyl groups at C-6 and/or C-3.

In related work, we are studying the applications of the resulting chitosan based on the use of amino group at C-2 and hydrophobic chains attached at C-6 and/or C-3 for controlled release systems for drugs/pesticides.

## Acknowledgements

The project was supported by National Science and Technology Development Agency of Thailand, National Metal and Materials Technology Center (MTEC), (MT-B-06-3D-09-102). The authors would like to thank Prof. Suwalee Chandkrachang for providing the raw chitosan material, and to Prof. Seiichi Tokura, Kansai University, Prof. Kohji Tashiro, Osaka University, Prof. Yasuyuki Tanaka, Mahidol University, Dr. Sei-ichi Aiba, Osaka National Research Institute, and Dr. T. X. Jaunet, Asian Vegetable Research and Development Center, for their help, suggestions, and comments. Appreciation is expressed to MTEC for solid-state  $^{13}\text{C}$  CP/MAS NMR measurements. The authors are indebted to Rigaku International Corporation, Japan, for partial support and collaboration. One of the authors (S.C.) would like to thank The Hitachi Scholarship Foundation for partial support of the present work.

## References

1. Richardson, S. C.; Kolbe, H. V.; Duncan, R. *Int. J. Pharm.* **1999**, *178*(2), 231-243.
2. Risbud, M. V.; Bhonde, R. R. *Drug Deliv* **2000**, *7*(2), 69-75.
3. Yamamoto, H.; Amaike, M. *Macromolecules* **1997**, *30*, 3936-3937.
4. Tomihata, K.; Ikada, Y. *Biomaterials* **1997**, *18*, 567-575.
5. Dumitriu, S.; Popa, M. I.; Cringu, A.; Stratone, A. *Colloid Polym Sci* **1989**, *267*, 595-599.
6. Matsushashi, S.; Kume, T. *J. Sci Food Agric* **1997**, *73*, 237-241.
7. Quarshi, M. T.; Blair, H. S.; Allen, S. T. *J. Appl. Polym. Sci.* **1992**, *46*, 255-261.
8. Sezer, A. D.; Akbuga, J. *J. Microencapsul.* **1999**, *16*(2), 195-203.
9. Kurita, K.; Yoshino, H.; Yokota, K.; Ando, M.; Inoue, S.; Ishii, S.; Nishimura, S. *I. Macromolecules* **1992**, *25*, 3786-3790.
10. Nishimura, S. I.; Kohgo, O.; Kurita, K. *Macromolecules* **1991**, *24*, 4745-4748.
11. Dung, P.; Milas, M.; Rinando, M.; Desbrieres, J. *Carbohydr. Polym.* **1994**, *24*, 209-214.
12. Kurita, K.; Ishii, S.; Tomita, K.; Nishimura, S. I.; Shimoda, K. *J. Polym. Sci.: Part A: Polymer Chemistry* **1994**, *32*, 1027-1032.
13. Chirachanchai, S.; Lertworasirikul, A.; Tachaboonyakiat, W. *Carbohydr. Polym.* **2000**, *46*(1), 19-27.
14. Ouchi, T.; Banba, T.; Matsumoto, T.; Suzuki, S.; Suzuki, M. *J. Bioact. Comp. Polymers.* **1989**.
15. Singh, D. K.; Ray, A. R. *J. Macromol. Sci.* **2000**, *40*(1), 69-83.
16. Allan, G. G.; Peyron, M. In *Chitin handbook*; Muzzarelli, R. A. A.; Peter, M. G., Eds.; European Chitin Society, 1997.
17. Allan, G. G.; Peyron, M. *Carbohydr. Res.* **1995**, *277*(2), 257-272.
18. Domard, A.; Cartier, N. *Int. J. Biol. Macromol.* **1989**, *11*(5), 297-302.
19. Nordtveit, R. J.; Varum, K. M.; Smidsrod, O. *Carbohydr. Polym.* **1994**, *23*, 253-260.
20. Aiba, S. I. *Carbohydr. Res.* **1994**, *265*, 323-328.
21. Andrady, A. L.; Torikai, A.; Kobatake, T. *J. Appl. Polym. Sci.* **1996**, *62*, 1465-1471.

22. Ulanski, P.; Rosiak, J. *Radiat. Phys. Chem.* **1992**, *1*, 53-57.
23. Lim, L. Y.; Khor, E.; Koo, O. *J. Biomed. Mater. Res.* **1998**, *43(3)*, 282-290.
24. Wenwei, Z.; Xiaoguang, Z.; Li, Y.; Yuefang, Z.; Jiaazhen, S. *Polym Degrad Stability* **1993**, *41*, 83-84.
25. Ebringerova, A.; Pruzinec, J.; Kacurakova, M.; Hromadkova, Z. *J. Appl. Polym. Sci.* **1989**, *38*, 1919-1928.
26. Chen, C. S. H.; Jankowski, S.; Brother, A. In *Irradiation of Polymers, Advances in Chemistry Series*; Gould, R. F., Ed.; American Chemical Society Washington, D.C., 1976, pp 240-255.
27. Miwa, A.; Ishibe, A.; Nakano, M.; Yamahira, T.; Itai, S.; Jinno, S.; Kawahara, H. *Pharm. Res.* **1998**, *15(12)*, 1844-1850.
28. Yoshioka, H.; Nonaka, K.; Fukuda, K.; Kazama, S. *Biosci. Biotechnol. Biochem.* **1995**, *95(10)*, 1901-1904.
29. How, N. C.; Chandkrachang, S.; Stevens, W. F. In *2<sup>nd</sup> ASIA PACIFIC CHITIN SYMPOSIUM*: Bangkok, 1996, pp 81-89.
30. Wang, W.; Bo, S.; Li, S.; Qin, W. *Int. J. Biol. Macromol.* **1991**, *13*, 281-285.
31. Ershov, B. G.; Isakova, O. V.; Rogoshin, S. V.; Gamzazade, A. I.; Leonova, E. U. *Dokl. Akad. Nauk SSSR* **1987**, *295(5)*, 1152.
32. Staab, H. A. *Angew. Chem. Internat. Ed.* **1962**, *1(7)*, 351-367.
33. Ferruit, P.; Vaccaroni, F. *J. Polym. Sci.: Polym. Chem. Ed.* **1975**, *13*, 2859-2862.
34. Morrison, R. T.; Boyd, R. N. In *Organic Chemistry*; Joraanstad, D.; Sharrock, C., Eds.; A Simon and Schuster Company: Englewood Cliffs, New Jersey, 1992, pp 31-32.
35. Grulke, E.A. In *Polymer Handbook*; Brandrup, J.; Immergut, E. H., Eds.; A Wiley-Interscience Publication: USA, 1989, pp 519-559.



**Chart Caption****Chart 1.** Chemical Structure of Chitin-Chitosan Copolymer

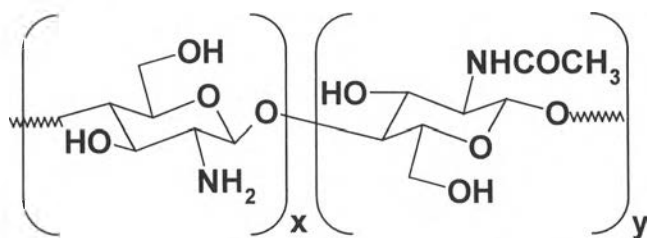
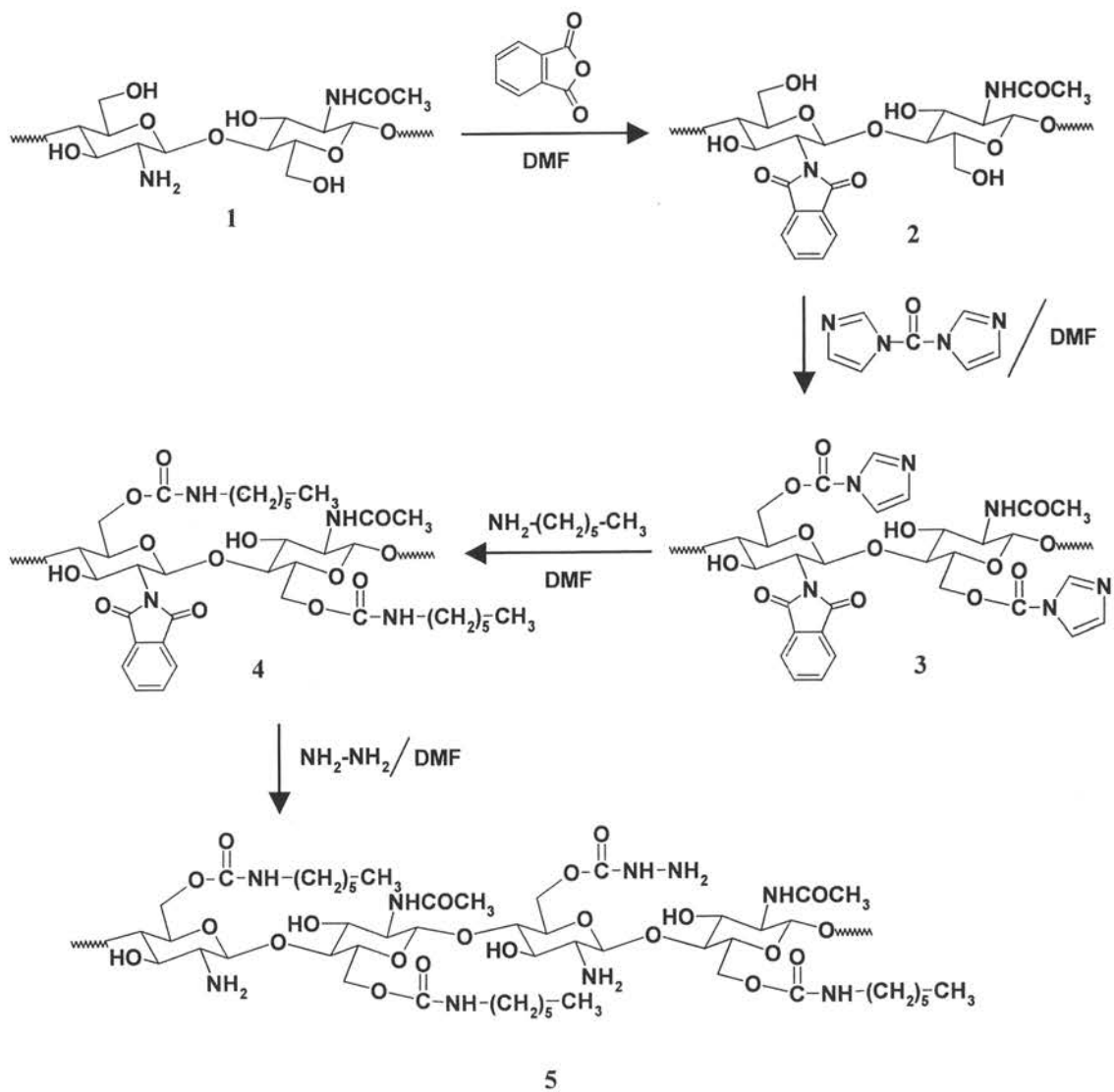


Chart 1. (Yoksan et al.)

**Scheme Caption**

**Scheme 1.** Preparation of  $\gamma$ -Ray Irradiated Chitosan Derivatives;  
N-Phthaloyl  $\gamma$ -Ray Irradiated Chitosan (**2**), N-Phthaloyl  $\gamma$ -Ray Irradiated  
Chitosan-CDI (**3**), N-Phthaloyl  $\gamma$ -Ray Irradiated Chitosan-CDI-(n-hexylamine) (**4**),  
and  $\gamma$ -Ray Irradiated Chitosan-CDI-(n-hexylamine) (**5**)



Scheme 1. (Yoksan et al.)

## Figure Captions

**Figure 1.** Molecular weight of  $\gamma$ -ray irradiated chitosan in solid state as a function of dose.

**Figure 2.** FT-IR spectra of compounds 1- 5.

**Figure 3.** UV absorbance at 293 nm of  $\gamma$ -ray irradiated chitosan as a function of dose.

**Figure 4.** X-ray diffractograms of compounds 1-3.

**Figure 5.** Deacetylation degree of chitosan as a function of dose determined by (a) indirect method integral ratios of amide I band ( $1655\text{ cm}^{-1}$ ) and hydroxy band ( $3450\text{ cm}^{-1}$ ) and direct methods (b)  $^1\text{H-NMR}$  and (c) acid hydrolysis-HPLC.

**Figure 6.** Comparison of FT-IR spectra of (a) chitosan starting material (81.8% deacetylation), (b) unirradiated chitosan-CDI, and (c)  $\gamma$ -ray irradiated chitosan (with dose 26.43 kGy)-CDI.

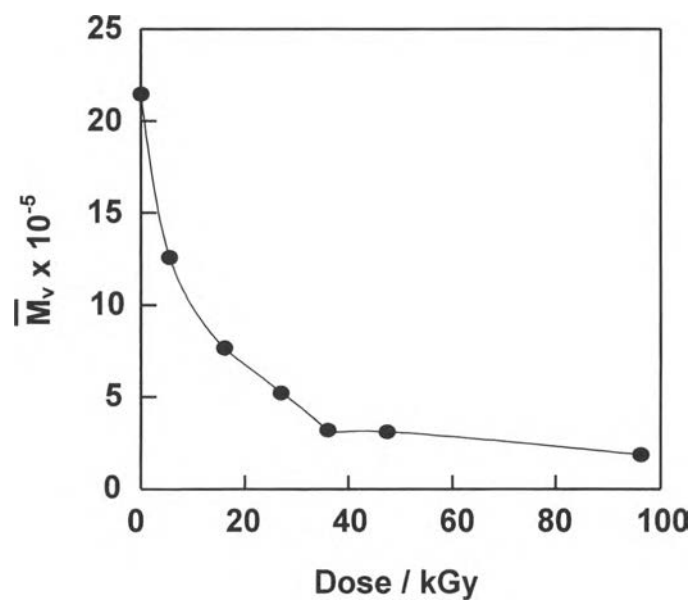


**Figure 1.** (Yoksan et al.)

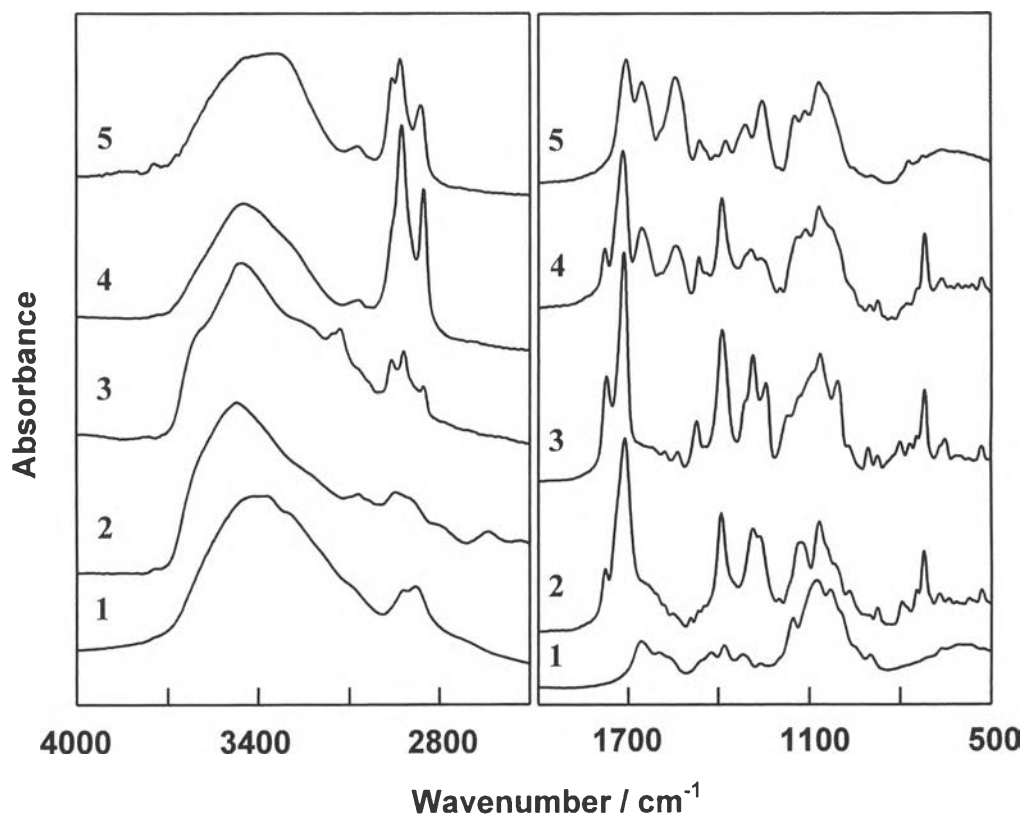


**Figure 2.** (Yoksan et al.)

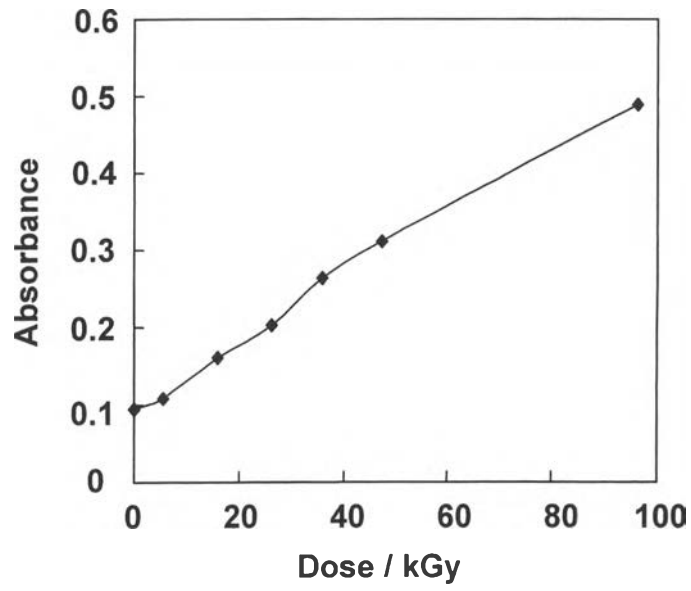


Figure 3. (Yoksan et al.)



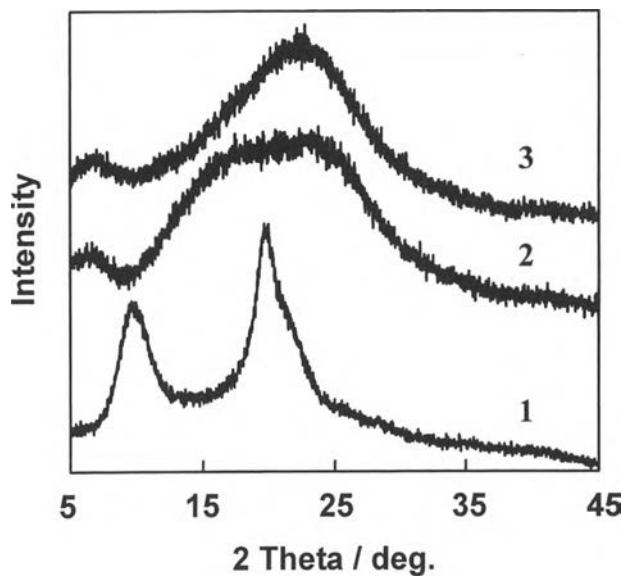


Figure 4. (Yoksan et al.)

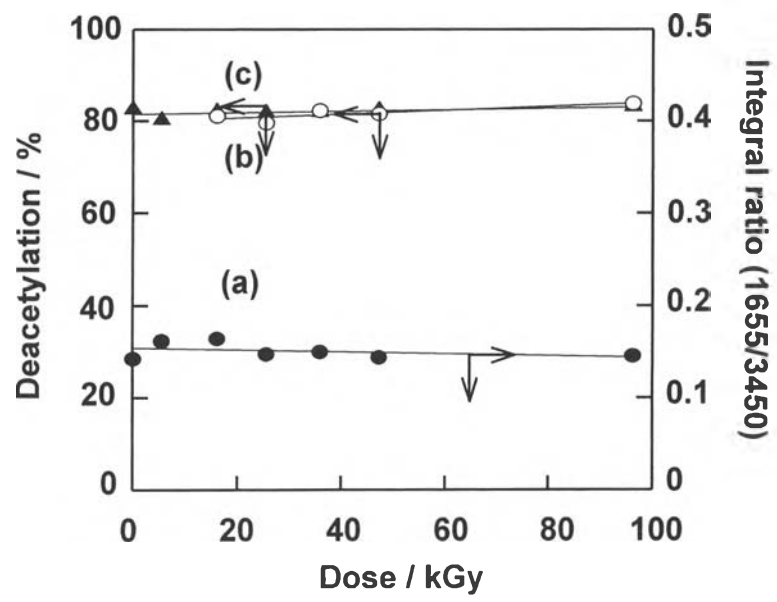


Figure 5. (Yoksan et al.)

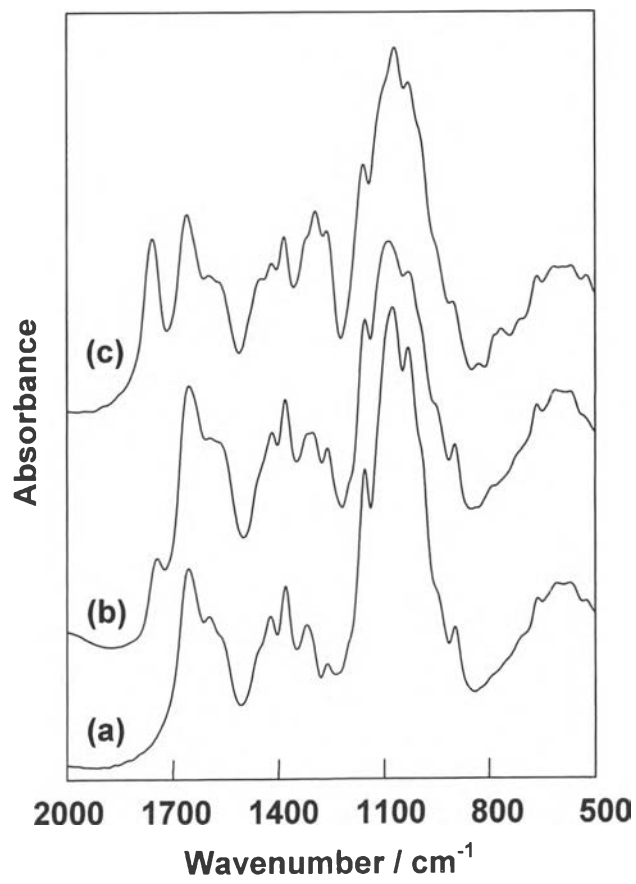


Figure 6. (Yoksan et al.)

**Table Captions**

**Table 1.**  $^{13}\text{C}$  CP/MAS NMR Chemical Shifts of Compounds **1- 3**.

**Table 2.** Solubility of Compounds **2- 5**.

type of carbon	chemical shift (ppm)			
	chitosan	1	2	3 <sup>a</sup>
C-1	105.3	104.3	100.4	100.5
C-2	57.7	57.7	57.0	57.3
C-3	75.6	75.6	73.2	73.8s 72.1w
C-4	83.4	82.6	80.5	79.6
C-5	75.6	75.6	73.2	73.8
C-6	61.2	61.0	64.6	64.6s 62.0w
CH <sub>3</sub>	23.8	23.6	23.3	23.5
C=O (acetamide)	174.1	174.2	169.1	169.2
benzene ring	-	-	131.1	131.1
imidazole	-	-	-	124.2 134.7

<sup>a</sup> s, strong peak; w, weak peak.

**Table 1.** (Yoksan et al.)

solvent	Solubility (mg/mL)			
	<b>2</b>	<b>3</b>	<b>4</b>	<b>5</b>
DMF	a	2.25	a	a
DMSO	a	2.71	2.01	a
DMAc	a	2.85	a	24.58 <sup>b</sup>
Pyridine	a	1.93	a	10.88 <sup>b</sup>
Toluene	0.07	0.21	0.17 <sup>c</sup>	0.01 <sup>c</sup>
Benzene	0.17	0.12	0.16 <sup>c</sup>	0.17 <sup>c</sup>
Xylene	0.02 <sup>c</sup>	0.05	0.12 <sup>c</sup>	0.04 <sup>c</sup>
Hexane	0.05	0.21	0.05 <sup>c</sup>	0.05 <sup>c</sup>
EtOAc	0.20 <sup>c</sup>	0.25	0.32 <sup>d</sup>	0.04 <sup>d</sup>
MEK	0.03 <sup>c</sup>	0.31	0.01 <sup>d</sup>	0.01 <sup>d</sup>
THF	0.21	0.07 <sup>c</sup>	0.15 <sup>d</sup>	0.03 <sup>d</sup>
Butanol	0.07 <sup>c</sup>	0.41	0.43 <sup>d</sup>	0.05 <sup>d</sup>

<sup>a</sup>Solubility for higher than 20 mg/mL. <sup>b</sup>Gel. <sup>c</sup>Partially swelled.  
<sup>d</sup>Obviously swelled.

**Table 2.** (Yoksan et al.)